Progress in the modelling of 3-D effects on MHD stability with the PB3D numerical code and implications for ITER

T. Weyens[1], A. Loarte[1], G. Huijsmans[2,3], J.M. Reynolds-Barredo[4]

[1] *ITER Organization, 13067 St. Paul Lez Durance Cedex, France* — [2] *Eindhoven University of Technology, Eindhoven, The Netherlands* — [3] *CEA Cadarache, IRFM, 13108 St. Paul Lez Durance Cedex, France* — [4] *Universidad Carlos* III *de Madrid, dpto de física, 28911 Leganés, Madrid, Spain*

1 Introduction

The theory of magnetohydrodynamics (MHD) is valuable because it leads to baseline considerations for toroidal magnetic configurations, even when the parameter ranges in which these configurations are situated often don't strictly satisfy the assumptions behind the MHD theory. The reason for this lies in the strong anisotropy of these configurations, where the dynamics perpendicular to the magnetic field lines is often indeed well-described by the theory, even though the direction parallel to the magnetic field lines is not. This work is situated in the study of *fluted* or **high-n** modes, which are normal modes that fit in the theory of MHD stability, that show very fast variation accross the magnetic field lines, as compared to the behavior along them. High-n MHD stability is important by itself as it can describe phenomena that are known to be important for the current and next generation of nuclear fusion devices, such as **ELM**s, which can be interpreted as due to two types of high-n instabilities: ballooning modes and peeling modes. In the view of studying these phenomena in enough detail, the two ingredients that this work combines within the world of high-n stability are the inclusion of a possible **vacuum perturbation**, which is necessary for peeling modes to exist in the absence of resistivity; and the correct treatment of **3-D effects**, which are important not only for stellarators, but also for tokamaks. An example thereof can be found in the well-known consequences that toroidal field (TF) ripples can have on confinement [Sai+07; Wey+17]; but also in the application of resonant magnetic perturbation (RMP) coils to control ELMs by destabilizing them [Eva+06]. After briefly summarizing the theory of ideal linear 3-D MHD stability and the advancements of the **PB3D** (Peeling-Ballooning in 3-D) code over the past year in 2, this work then treats its application to the study of 3-D ballooning stability when applying RMPs in tokamaks in 3 and 4. Finally, in section 5, conclusions are phrased as well as the plans for future work.

2 Ideal linear 3-D MHD stability and PB3D

Normal modes, whose time behavior is described mathematically through a complex frequency ω, are solutions to the equations that describe stability of perturbations $\boldsymbol{\xi}$ of time-invariant equilibrium configurations. High-n modes, furthermore, can be described appropriately through an angular Fourier series combined where the amplitudes of the harmonics depend on some flux function, commonly chose to be the poloidal or toroidal flux. Furthermore, by introducing the field-line label $\alpha = \zeta - q\theta$, where θ and ζ are poloidal and toroidal angles in which the magnetic field $\mathbf{B}$ appears straight, the requirement for flutedness translates to a condition $nq - m \ll n,m$ where the poloidal and toroidal mode numbers, respectively m and n, are both $\gg 1$:

$$\boldsymbol{\xi}(\mathbf{r},t) = \sum_{n,m} \hat{\boldsymbol{\xi}}_{n,m}(\psi)\, e^{\mathrm{i}\omega t} e^{\mathrm{i}[n\alpha - (nq-m)\theta]} . \tag{1}$$

By introducing the Harmonics $\hat{\boldsymbol{\xi}}_{n,m}$ in the quadratic form that describes MHD stability [GP04, sec.

6.6], it can be seen that two out of three vectorial components can be minimized with respect to the third: one by eliminating sound waves and the other by avoiding the fast magnetosonic waves. After finally performing Euler minimization, the result is a coupled system of second-order ordinary differential equations for the resulting normal components $X_{n,m} = \nabla\psi \cdot \hat{\boldsymbol{\xi}}_{n,m}$, which after discretization leads to a generalized Eigenvalue problem. This is the problem that PB3D tackles, with the help of a variety of specialized libraries, such HDF5, Slepc and Petsc and MPI. It has been verified with MISHKA [Mik+97] and COBRA [San+00] for ballooning studies and has subsequently matured into a fast, user-friendly, fault tolerant and extensively documented code with advanced post-processing capabilities.

The PB3D code, its documentation and source code can be found at its homepage:

`http://pb3d.github.io/`

3 RMP free-boundary ITER equilibria

The ITER RMP coils, portrayed in figure 1, are arranged in three rows, of which the phases can be controled independently. Using this, the alignment of the magnetic perturbation induced by the coils can be varied and its effects on ELM stability can be studied.

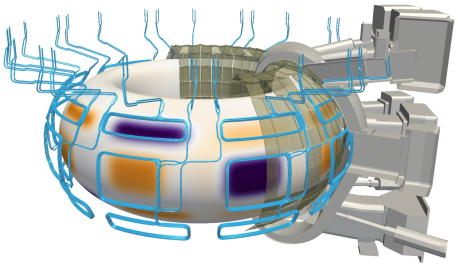

Fig. 1: ITER RMP coils and induced field disturbances.

In a first step, in this work, the VMEC numerical code [Hir83] was used in free-boundary mode to calculate equilibrium configurations that result from detailed and realistic given currents in the poloidal field (PF) coils, toroidal field (TF) coils and vertical stability (VS) coils, combined with assumed flux function profiles for the toroidal current and the pressure. The case of interest here was the full magnetic field of 5.3T and full toroidal current of 15MA reference case, which corresponds to Q=10, with 33MW of NBI and 20MW of ECRH heating.

Subsequently, the RMP coil currents were fixed at 90kA current and the phase differences between, on the one hand, the top and the middle rows of RMP coils, and the bottom and the middle rows on the other hand, were scanned in steps of 15° from 0° to 105°.

For each of 64 resulting equilibrium configurations, the maximum displacement of the plasma boundary as compared to the corresponding axisymmetric version without TF ripple and RMP perturbation, was then investigated. The resulting displacements at the X-point and at the outer midplane are summarized in figure 2. From the figure, it can be seen that there is strong correlation between the displacements at the X-point and the outer midplane, but that the maximum occurs at larger top coil row phase difference for the outer midplane: around (60°, 90°) top-bottom phases versus (60°, 60°) top-bottom phases. Furthermore, these results can be compared directly to the ones from [Li+17] where MARS-F simulational results are presented: The displacement that results from the VMEC equilibria has a similar profile to the MARS-F equilibria, but the absolute value is larger for the MARS-F code, which solves the linearized, resistive, full MHD equations in toroidal geometry with inclusion of toroidal flow, as opposed to VMEC's ideal treatment.

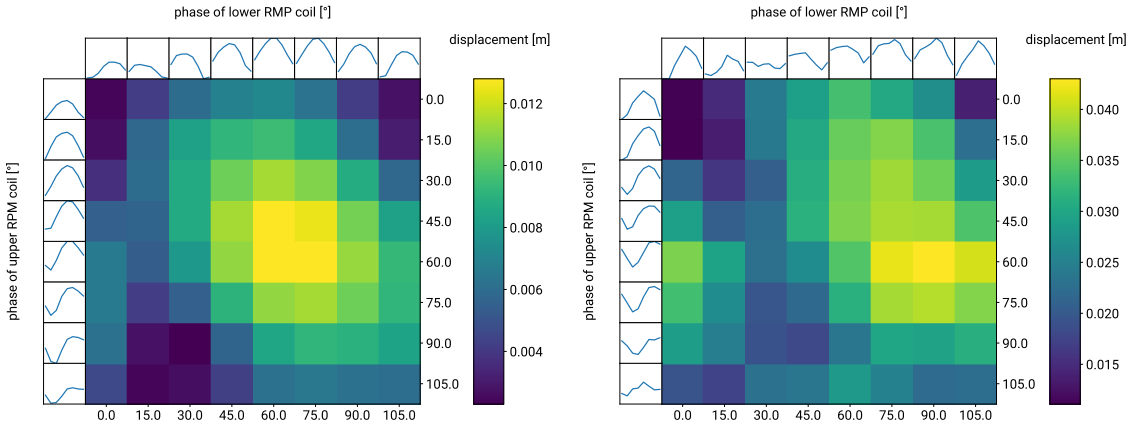

(a) Displacement at X-point. **(b)** Displacement at midplane.

Fig. 2: The maximum displacements induced by TF coils and RMP coils at the X-point (**a**) and the outer midplane (**b**) for 8×8 configurations with varying top and bottom coil phases, relative to the middle coil row.

4 RMP effects on ballooning stability in tokamaks

Using the PB3D code, the 3-D ballooning stability of the equilibria discussed in the previous section was then analyzed. Since the ITER configurations generally lie firmly in the peeling-dominated region, due to the presence of strong bootstrap currents, however, two approaches were attempted to be able to focus on ballooning stability.

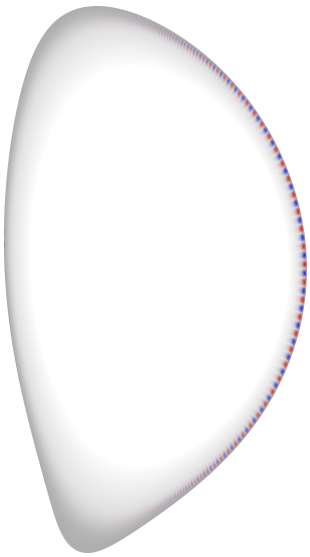

Fig. 3: Ballooning mode structure of $X = \nabla\psi \cdot \hat{\boldsymbol{\xi}}$ for zero bootstrap current modified 15MA/5.3T case and shaded pressure profile.

In the first approach, the bootstrap current was gradually removed, which physically corresponds to the physical situation where the colliosionality is higher. As discussed in [Mag+13, fig. 24], lowering the pedestal current fraction while keeping the pedestal pressure constant decreases stability for the 15MA/5.3T ITER reference case, and this is also what was observed with the PB3D simulations: Typical ballooning modes appeared for axisymmetric equilibria when the pedestal current was lowered by more than half compared to the reference case. Figure 3 shows an example for zero bootstrap current. However, this approach leads to strongly modified shapes for the last flux surface when computing the free-boundary RPM equilibria: On the one hand, the equilibria became much less D-shaped due to the lower Lorenz forces exerted by the poloidal field coils in the outer flux surfaces that now carry less current, and, on the other hand, the Shafranov shift was increased because of the higher l_i. For these reasons, we opted for an alternative approach to study ballooning stability.

For the second approach to study ballooning stabillity, the plasma perturbation was held fixed to zero at the plasma edge and the bootstrap current profile was left untouched. This has the effect of stabilizing the current-driven normal modes, as ideal peeling modes require perturbation of surrounding vacuum to exist. The resulting modes are still partially driven by parallel current, but also by the unfavorable curvature that drives ballooning modes and is the modification of this stability by RMP perturbations that we are interested in.

The main results are summarized in figure 4, which shows the most unstable growth rate for the 8×8 orientations discussed in section 3. The most striking feature of this plot is the appearance of a band of enhanced instability that exists only for lower coil phases around 75° to 90°, where the upper coil phase has only a second order effect. It can be seen, furthermore, that the maximum enhancement of instability corresponds to the positions of maximum displacement of the midplane seen in figure 2.

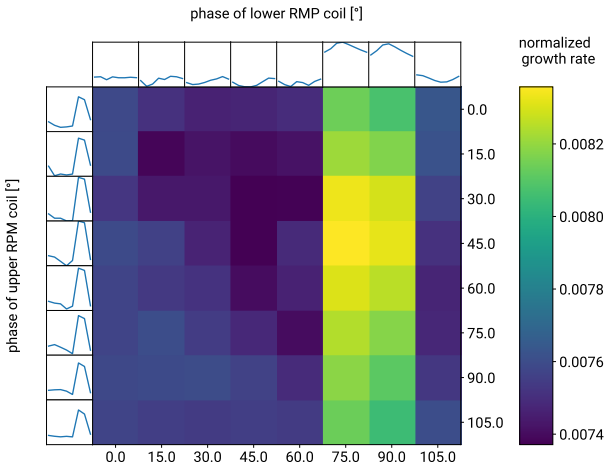

Fig. 4: growth rate $\gamma = \mathscr{R}(\omega)$ for 8×8 RMP equilibrium configurations, together with horizontal and vertical spark lines that describe the variation in the respective row or column.

At the same time, however, the effect of field-line alignement seen in that figure, is not at all visible in this figure. This can be explained by the observation that all the modes with enhanced growth rate, corresponding to the lower coil phases of 75° and 90° are of a different nature than the others: They are of the internal tearing-like nature, localized around normalized poloidal flux $\psi \approx 0.89$, as opposed to modes that show a combined peeling and ballooning nature, but with the mode fixed at the edge. These latter modes, which are less unstable, in fact are not different from the ones found in the axisymmetric configurations, so it is really the appearance of internal tearing-like modes that is the result of the deformations of the plasma by RMP coils. This fits in the physical picture built up in [NB03] where the effect of normal displacements of the plasma surface is directly linked to the appearance of internal islands. However, more work is needed to assess this statement.

5 Conclusions and future work

The progress of the PB3D numerical code (`http://pb3d.github.io/`) was discussed, including the fact hat it has matured into a user-friendly, fault-tolerant and extensively documented code. Afterwards, its application to study the effects of RMPs on ballooning stability, where the normal modes cannot move the edge, has shown the appearance of internal tearing-like modes, that are more unstable than the other modes, when the lower RMP coils phase was 75° or 90°.

For future work, the first step, which is currently being completed, is the inclusion of possible vacuum energy perturbation by normal modes that perturb the plasma surface. The axisymmetric implementation has been verified with MISHKA and the full 3-D implementation will follow soon. This will allow us to complete the study of RMP effects on stability with a greater space of possible normal modes. For ITER, which operates strongly in the peeling regime, this will benefit the applicability of the results.

ITER is the Nuclear Facility INB no. 174. The views and opinions expressed herein do not necessarily reflect those of the ITER Organization

References

[Eva+06] Todd E Evans et al. In: *Nature Physics* 2.6 (2006), pp. 419–423.
[GP04] J. P. Hans Goedbloed and Stefaan Poedts. Cambridge: Cambridge University Press, 2004.
[Hir83] S. P. Hirshman. In: *Physics of Fluids* 26.12 (1983), p. 3553.
[Li+17] L. Li et al. In: *Plasma Physics and Controlled Fusion* 59.4 (2017).
[Mag+13] P. Maget et al. In: *Nuclear Fusion* 53.9 (2013), p. 093011.
[Mik+97] A. B. Mikhailovskii et al. In: *Plasma Physics Reports* 23.10 (1997), pp. 844–857.
[NB03] Carolin Nührenberg and Allen H. Boozer. In: *Physics of Plasmas* 10.7 (2003), pp. 2840–2851.
[Sai+07] G. Saibene et al. In: *Nuclear Fusion* 47.8 (2007), pp. 969–983.
[San+00] R. Sanchez et al. In: *Journal of Computational Physics* 161.2 (2000), pp. 576–588.
[Wey+17] T Weyens et al. In: *44rd European Physical Society Conference on Plasma Physics (EPS)*. 2017, O4.128.